Available online at www.sciencedirect.com

ScienceDirect

Journal of Natural Gas Geoscience 4 (2019) 47−62

http://www.keaipublishing.com/jnggs

Original research paper

Microfacies characteristics and reservoir potential of Triassic Baikouquan Formation, northern Mahu Sag, Junggar Basin, NW China

Xinchuan Lu [a,*], Dong Sun [b], Xiangyang Xie [c], Xin Chen [d], Shuncun Zhang [a], Shengyin Zhang [a], Guoqiang Sun [a], Ji'an Shi [a]

[a] *Key Laboratory of Petroleum Resources, Gansu Province/Key Laboratory of Petroleum Resources Research, Institute of Geology and Geophysics, Chinese Academy of Sciences, Lanzhou 730000, China*

[b] *Research Institute of Petroleum Exploration & Development-Northwest, PetroChina, Lanzhou, 730020, China*

[c] *School of Geology, Energy, and Environment, Texas Christian University, Fort Worth, TX, 76129, USA*

[d] *Fengcheng Oilfield Operation District, Xinjiang Oilfield Company, PetroChina, Karamay, 834000, China*

Received 19 October 2017; revised 21 December 2018
Available online 21 March 2019

Abstract

By using data such as lithology, thin sections, sedimentary structure, particle size, logging facies signs, mercury intrusion, porosity and permeability from 34 wells, 11 types of sedimentary microfacies were divided in this study. Upon analysis, sedimentary microfacies exert significant control on reservoirs, and high quality reservoirs are primarily developed with the following sedimentary microfacies: gray sandy conglomerate in underwater distributary channels microfacies of fan delta fronts sub-facies, river-estuary dams and gray sandstones of distal bars on the front edge of the fan delta that have strong hydrodynamic conditions and good stability. Relatively good reservoirs are primarily distributed in the braided channel in fan-delta plains with brown sandy conglomerates, main channel of underwater distributary channels on the front edge of the fan delta with gray conglomerates and underwater distributary channel ends on the front edge of the fan delta with gray fine sandstones. With the stable tectonic background, Triassic sedimentary microfacies in the Mahu sag control the distribution and development of reservoirs. Therefore, sites of high quality reservoirs can be predicted by sedimentary microfacies, and this study provides guidance for oil and gas exploration.

Keywords: Microfacies; Reservoir; Mahu sag; Junggar Basin

1. Introduction

The Junggar Basin is one of petroliferous and superimposed basins in northwest China [1−3] (Fig. 1). Research and activities of hydrocarbon exploration and development in this basin have been mainly focused on detailed studies about the depositional system and reservoir characterizations in the northwestern margin of the Junggar Basin. They have been conducted over the last decade, in particularly, diagenesis history, facies and sub-facies characteristics of the fan delta, and reservoir property and its controls of distribution of hydrocarbon [4−10]. However, characteristics of microfacies and their controls on reservoir rocks, such as pore structure, property, and variation within different sedimentary environments, have not been thoroughly documented.

In this study, we focus on Triassic Baikouquan Formation in the northern Mahu sag, northwestern margin of the Junggar Basin to systematically document its types, distribution, and potential impacts on reservoir properties (Fig. 1).

The Triassic Baikouquan Formation of the Mahu Sag represents the transgressive period, leading to the decreasing of

* Corresponding author.
E-mail address: xclu@lzb.ac.cn (X. Lu).
Peer review under responsibility of Editorial office of *Journal of Natural Gas Geoscience*.

https://doi.org/10.1016/j.jnggs.2019.03.001

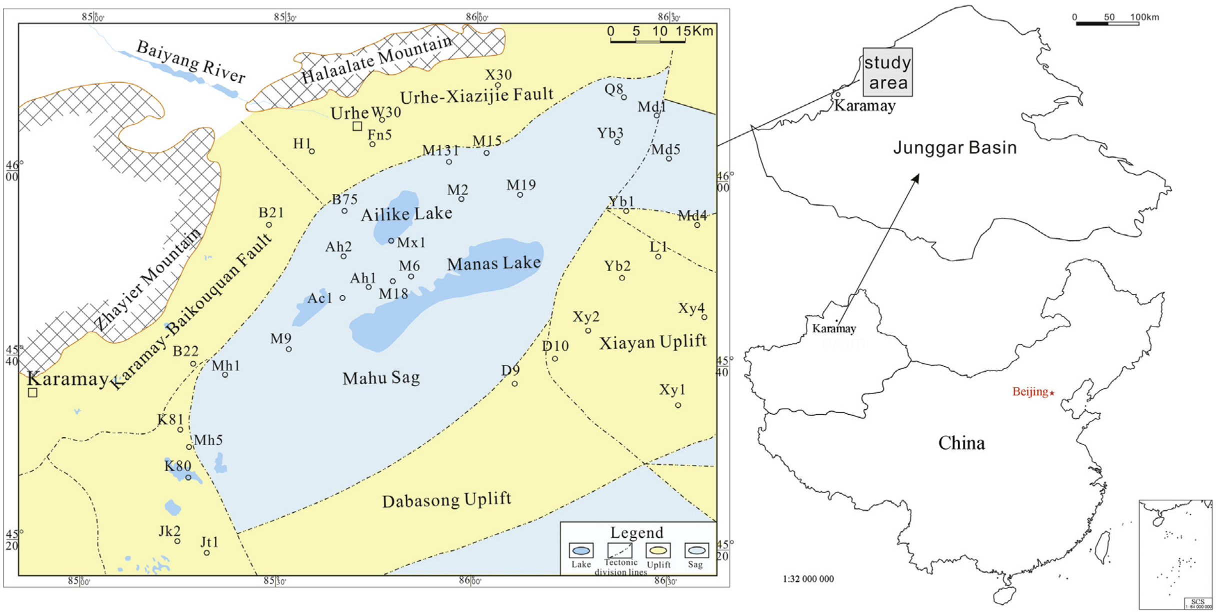

Fig. 1. Tectonic position of the Junggar Basin and location of the study area.

fan-delta plain areas and increasing fan delta front areas [4,5]. Studies show that fans in the Muhu Sag are well-developed and superimposed [5], and are mainly dominated by conglomerate and pebbly medium-coarse sandstone and mudstone.

Therefore, this study reveals the distribution characteristics of reservoirs with different sedimentary microfacies, to provide a theoretical basis and method for establishing a depositional model in an alluvial fan-fan delta-lacustrine depositional system, and to determine the future exploration direction of high-quality reservoirs.

2. Geological setting and stratigraphy

During the Late Paleozoic era, the Junggar-Turpan plate subducted and collided with the Kazakhstan plate, resulting in a collisional uplift zone and thrust the belt along the northwest margin of the Junggar Basin [3,11]. From south to north, the Junggar Basin can be divided into the north-south striking Hongche fault zone, north-east striking Kebai fault zone and west-east striking Wuxia fault zone [3,12]. In the Early Permian Jiamuhe Period, the majority of the Junggar Basin was under a compressional stress field of the foreland basin, except its northwest margin that remained as a rift setting. Starting from the Early Permian Jiamuhe Period to the Late Permian Urhe Period, deposits of the fan delta from the northwest edge advanced gradually from the basin margin to the basin center, and overall areas of fan bodies continued to extend and showed obvious mobility [4]. Until the Triassic era, the Junggar Basin began to transit from foreland basin to intra-continental depression, and syn-depositional thrusting activities along various Triassic tectonic belts led to the development of sedimentary fan bodies in different structural belts [5,13].

The Mahu Sag is part of the central depression of the Junggar Basin (Fig. 1). It was mainly developed in the Middle to Late Permian era and completed in the Triassic era, and then transformed to a sag basin [3,14–16]. These tectonics are more developed when strata are deeply buried. However, in shallow buried strata the tectonics are monoclinic tectonics declining to the southeast direction, and some places developed low-angle platform, anticline or nose tectonics [17–19]. Triassic strata in the Mahu Sag can be divided into three formations from the bottom to the top: the Baikouquan Formation (T_1b), the Karamay Formation (T_2k) and the Baijiantan Formation (T_3b). The Baikouquan Formation can be further divided into three stages as the 1st (T_1b_1), the 2nd (T_1b_2), and the 3rd (T_1b_3) members of the Baikouquan Formation from the bottom to the top (Fig. 2).

The total thickness of the Baikouquan Formation is approximately 200 m and the thickness of T_1b_1 is approximately 50 m. It mainly consists of fan-delta plain sub-facies with fan-delta plain channel and fan-delta plain river interchannel microfacies, and its lithologies are primarily fine-middle conglomerates that are then inverted into conglomerate and sandy conglomerates from the bottom to the top, where cross bedding and groove bedding are visible (Fig. 2). At the top of the T_1b_1 there is a non-conspicuous erosion surface where coarse sandstone deposits are located on the fine conglomerates, followed by the development of cross bedding in the pebbly sandstone and fine sandstone, and ripple bedding in siltstone and muddy siltstone. The thickness of T_1b_2 is approximately 80 m. It is primarily composed of fan delta front sub-facies with the fan delta front channel and delta front interchannel microfacies. It is dominated by conglomerate, mudstones and fine sandstones. The lower part of the fan delta front consists of high-angle inclined bedding of middle-fine conglomerate and sandy conglomerate, while the upper part is mainly composed of low-angle inclined bedding of siltstones and a mudstone interlayer; the fine and middle-coarse

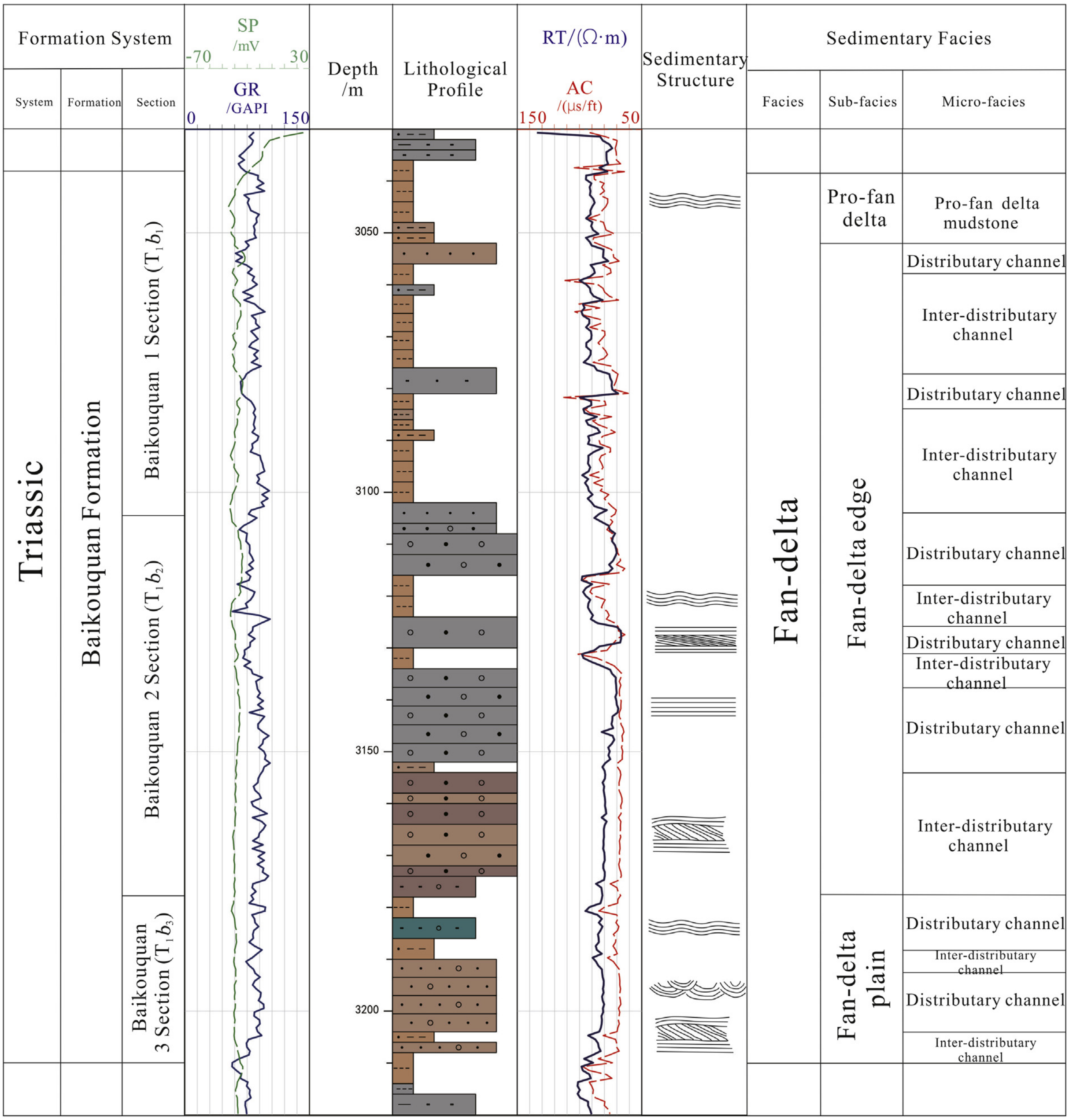

Fig. 2. Integrated histogram for the sedimentary facies for Well Ma13.

conglomerates are a scour contact with the cross bedding. The thickness of T_1b_3 is approximately 70 m. Its facies are primarily fan delta front sub-facies and profan delta sub-facies, and its lithology includes interbedded mudstone and thin siltstone with ripple bedding and horizontal bedding (Fig. 2).

3. Research methods

Core observation was done at the core center of Xinjiang Petroleum Company, Karamy city. Thin sections were examined under a Zeiss microscope at the Test Center of PetroChina Xinjiang Petroleum Company. The data of grain size, porosity, permeability and well log curves were collected from the PetroChina Xinjiang Petroleum Company.

Via integrated core observation, lithology, thin section, sedimentary structure and texture, particle size and well logging curves, the north Mahu fan delta was divided into 11 sedimentary microfacies. The physical property characteristics of microfacies of various reservoirs were analyzed by the porosity, permeability and mercury intrusion curve.

4. Sedimentary microfacies and their characteristics

The study of sedimentary microfacies is mainly based on facies markers and vertical sequence combinations. A total of 11 types of microfacies was identified in the Mahu Sag based on sedimentary sequences, rock texture, and well log signatures.

The fan delta in the northern Mahu area is controlled by turbidity current and normal river flow, where the flooding period is primarily driven by gravity flow or debris-flow, while the normal water period is primarily driven by tractive current. As a result, the northern Mahu fan delta has numerous genetic types, such as debris-flow deposition, braided channel filling and underwater diversion channel deposition. There are three sub-facies in the northern Mahu fan delta: the fan delta plain, the fan delta front and the pro-fan delta. The fan delta plains over the water surface can be further divided into debris-flow facies with conglomerate, braided channel facies with conglomerate and plain inter-channel sandy mudstone microfacies with sandy mudstone; the fan delta fronts can be divided further into six sedimentary microfacies, including underwater main channel facies with gravel, underwater channel facies with conglomerate, underwater inter-channel facies with sandy mudstone, underwater river end sandstone microfacies and river mouth bar-distal bar sandstone microfacies; and the pro-fan delta can be divided into pro-fan delta siltstone microfacies and pro-fan delta mudstone microfacies.

4.1. Debris-flow of the fan-delta plain with conglomerate microfacies

The debris-flow microfacies in the fan-delta plain with conglomerate are located at the top of the fan delta which is above the water surface. They have structural features of an alluvial fan mixed with sedimentary characteristics of gravity flow and mudslides during the flooding period. Major signatures include mixed accumulation of gravel, sandy conglomerate, and brown, light brown and mottled colored mudstone. The sedimentary structural features include erosion-filling structures, high-angle oblique bedding, and thick-layered massive structures in the conglomerate. Overall, they are characterized by stacked massive beddings with a visible erosional surface on the bottom. Grain size of debris-flow conglomerate facies in the fan delta plain is relatively coarse, and its probability curve of grain size is of a one-stage style, and the average and median sizes are −0.74 φ and −0.89 φ, respectively (Fig. 3). Sorting is poor to very poor with high matrix content, and no imbrication is presented. It is characterized by deposits of density flow, which reflects the gravity flow in an unstable, turbulent environment. Its electrical well log curves (GR) show a high magnitude, box-shape (Fig. 3). The displacement pressure curve of the mercury intrusion is 0.77 MPa, the average pore-throat radius is 0.07 μm, and the efficiency of mercury withdrawal is 25.54. The porosity range of the debris-flow facies is 6.3%−10.7% with an average of 8.87%; the permeability range is 0.53×10^{-3}-396.28×10^{-3} μm^2 with an average of 8.34×10^{-3} μm^2 (Fig. 3).

4.2. Fan delta plain braided channel with sandy conglomerate microfacies

The fan-delta plain braided river microfacies is primarily composed of brown and mottled sandy conglomerate and sandstone. The composition of those conglomerates is complicated, with a mixture of volcanic rocks and clastic rocks. They are poorly sorted and moderately rounded with sub-rounded to sub-angular shapes. Mostly are particle-supported and interval of grains is filled by a matrix.

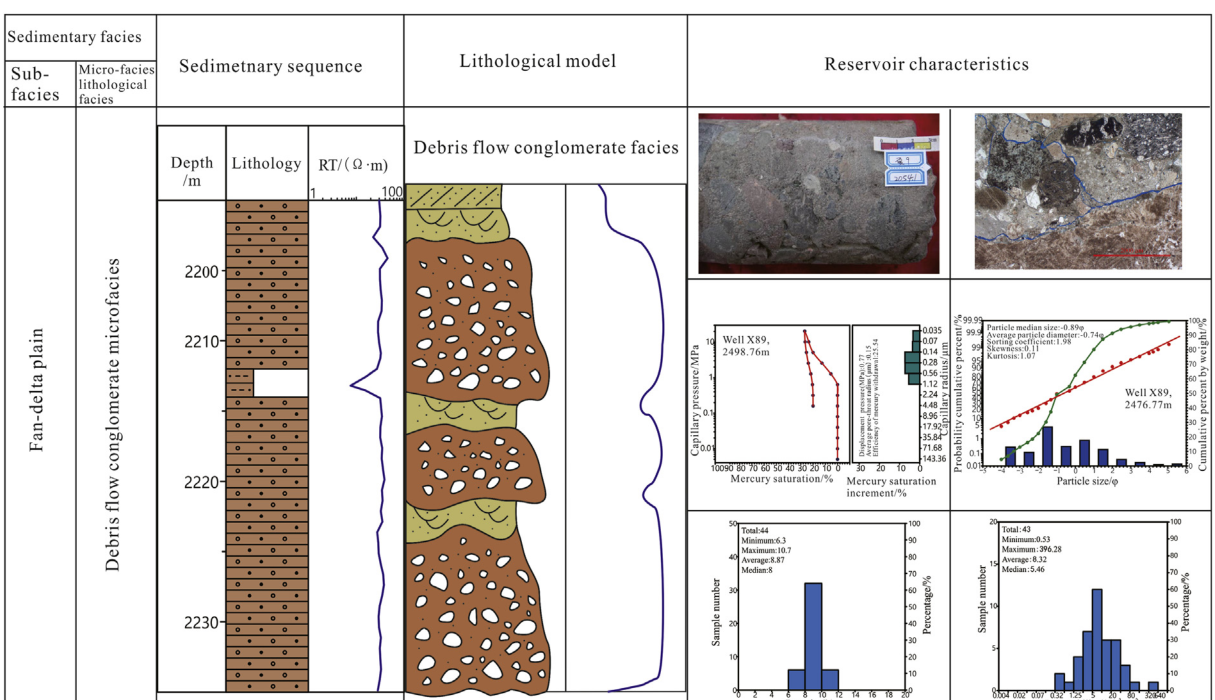

Fig. 3. Sedimentary characteristics of the debris-flow microfacies in the fan-delta plain with conglomerate rock.

Oblique, trough-cross, and graded beddings are common in lenticular sand bodies (Fig. 4). In addition, there are erosional surfaces within the sandy conglomerate, reflecting the frequent scouring and filling processes of floods. The resistivity curve has an overall box style overprinted with weak tooth-like, moderate magnitude and cyclic features. Each cycle is tooth-like, and forms a vertical stack of multiple tooth-like shapes with a box style. The probability cumulative curve of the grain size displays a two-stage style, and the average particle size is -1.50φ ($\varphi = -\log_2^d$, d stands for particle diameter mm) and the median size is -2.03 φ. The mercury intrusion curve indicates a crooked pore and thin throat distribution. The displacement pressure is 0.25 MPa, and the average pore-throat radius is 0.48 μm. In addition, the efficiency of mercury withdrawal is relatively good at 15.85. Overall, the fan-delta plain braided river conglomerate facies has good reservoir properties. It has relatively high porosity and permeability and is a favorable reservoir microfacies in the Mahu Sag. The range of porosity is 6.81%−12.90%, with an average porosity of 10.78%, and the range of permeability is 0.38 × 10^{-3}

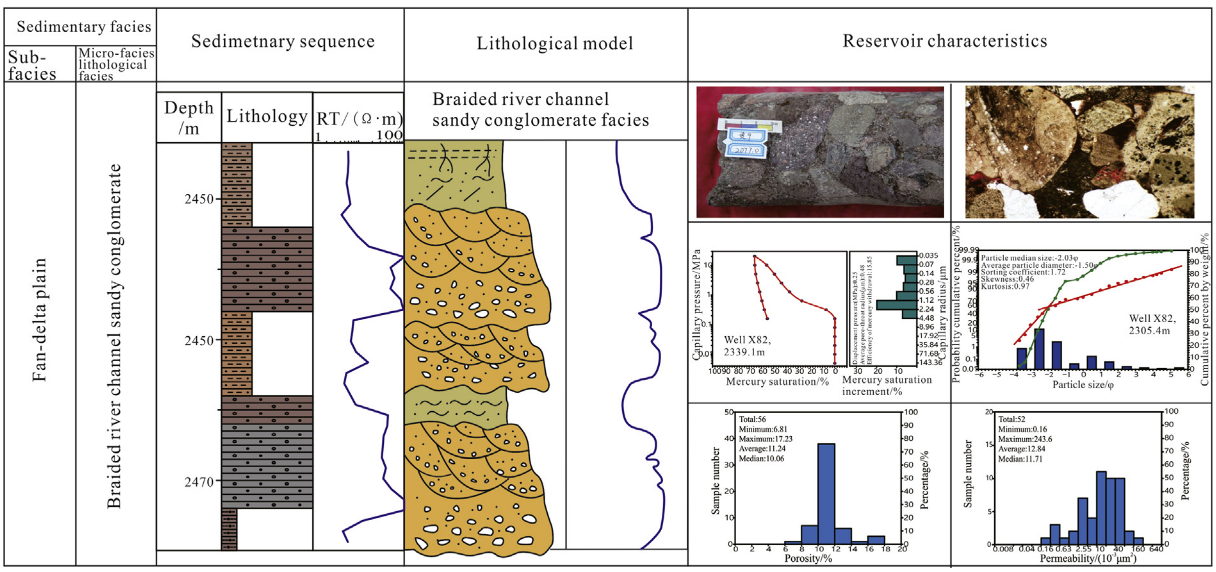

Fig. 4. Sedimentary characteristics of the fan-delta plain braided river microfacies with sandy conglomerate.

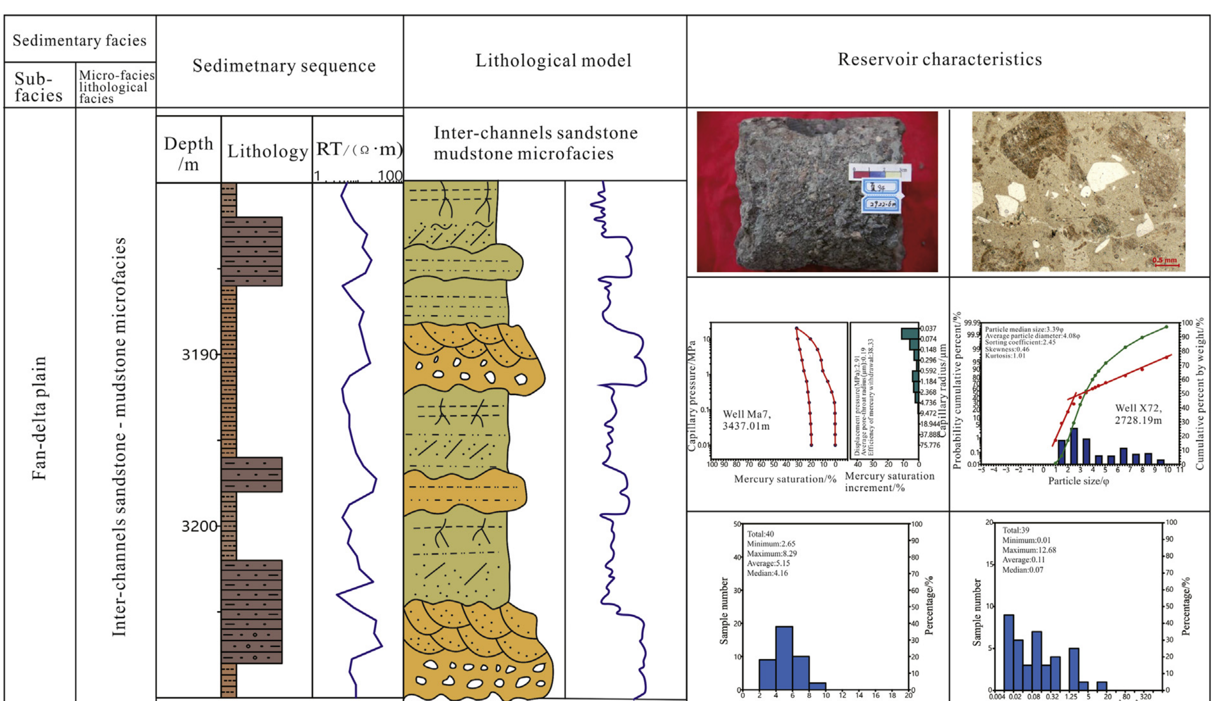

Fig. 5. Sedimentary characteristics of the fan-delta plain river intercourse microfacies with sandstone-mudstone.

-243.60 × 10^{-3} μm^2, with an average of 14.07 × 10^{-3} μm^2 (Fig. 4).

4.3. Fan delta plain inter-channels sandstone-mudstone microfacies

Fan-delta plain inter-channels sandstone-mudstone microfacies are formed by the deposition of overflowing water from the side edge of channels. It is primarily brown, palm-brown, and mottled mudstone, argillaceous siltstone and siltstone. The sorting of sandstone is moderate with a high matrix content. Most of strata have lenticular and wedge shapes with parallel bedding. The probability cumulative curve of the grain size shows an atypical two-stage style. The well-logging curve exhibits tooth-like and box-like shapes with a low magnitude. Fine particles are dominated in these microfacies, with the average particle size at 4.08 φ and the median size at 3.39 φ. The mercury intrusion curve shows that the mercury withdrawal efficiency is 38.33. The pore-throat radius belongs to micro-pores with an average at 0.19 μm. The average porosity is 5.15%, and the average permeability is 0.11 × 10^{-3} μm^2. Compared with the adjacent braided channel, the properties of the fan-delta plain inter-channels sandstone-mudstone microfacies are relatively poor (Fig. 5).

4.4. Underwater main channel conglomerate microfacies in the fan delta front

The underwater main channel conglomerate microfacies on the fan delta front is located at the underwater zone of the fan delta. This microfacies is the main body of the fan-delta deposition and has the most developed part of sand bodies with the largest range of distribution. The lithology is mostly poorly sorted (with a sorting coefficient of 1.75), sub-rounded to sub-angular, gray to green and mottled conglomerate, sandy conglomerate and coarse sandstone. In the thick-layered conglomeratic rock bodies, there are visible large oblique trough-cross beddings. The resistivity curve combination exhibits tooth- and bell-like and box-like shapes. The probability curve of the grain size has the typical traction flow characteristics with a two-stage style. The grain sizes range from -4φ to 6 φ, averaging at 1.26 φ. The range of porosity is 5.3%–23%, with an average at 9.06%, and the range of permeability is 0.08 × 10^{-3}-128.67 × 10^{-3} μm^2, with an average at 2.51 × 10^{-3} μm^2. The mercury intrusion curve shows the displacement pressure is 1.12 MPa, and the efficiency of mercury withdrawal is relatively good (46.80). Overall, the main channel conglomerate microfacies in the fan delta front shows strong reservoir heterogeneity. Its porosity is relatively good, but its permeability varies spatially and belongs to moderate-pore and fine-throat categories (Fig. 6).

4.5. Underwater channel sandy conglomerate microfacies in the fan delta front

The underwater channel sandy conglomerate microfacies is formed in the fan delta front. When the fan delta advances toward the lake along with the delta plain sub-facies braided river course, the channels become wide and shallow as the hydrodynamics weaken, and the branches gradually increase to form underwater distributary channels. Therefore, the vertical and horizontal heterogeneity of this facies is strong. The

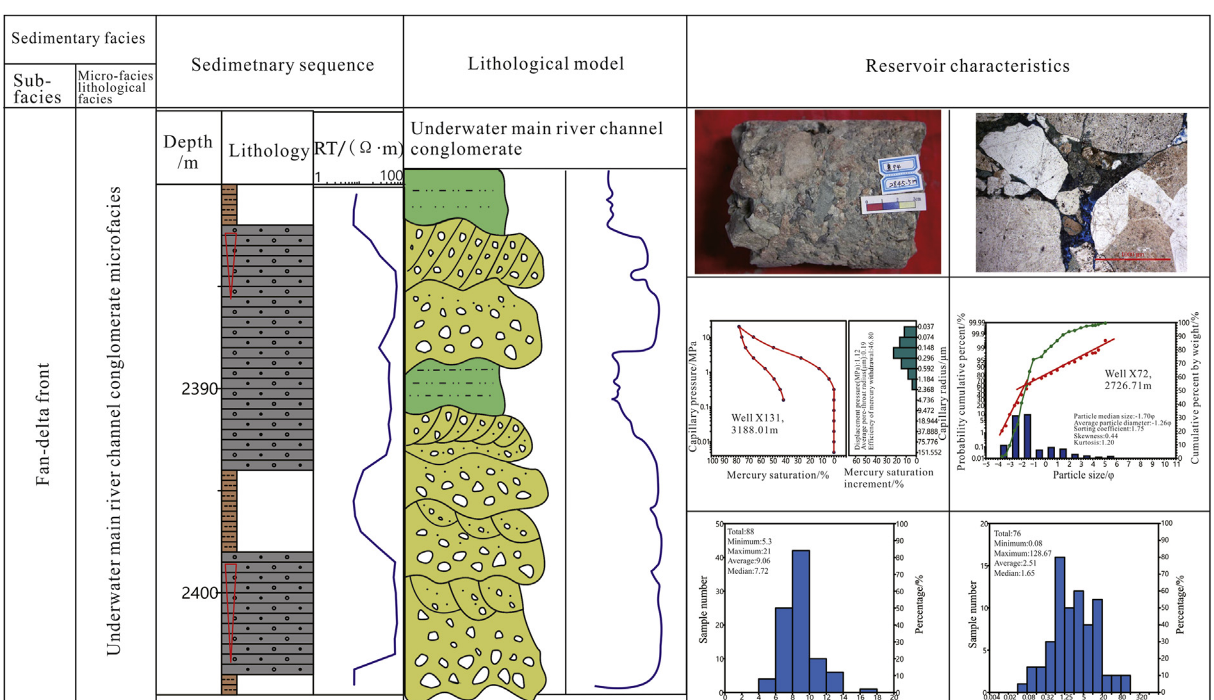

Fig. 6. Sedimentary characteristics of the underwater main river course conglomerate microfacies in the fan delta front.

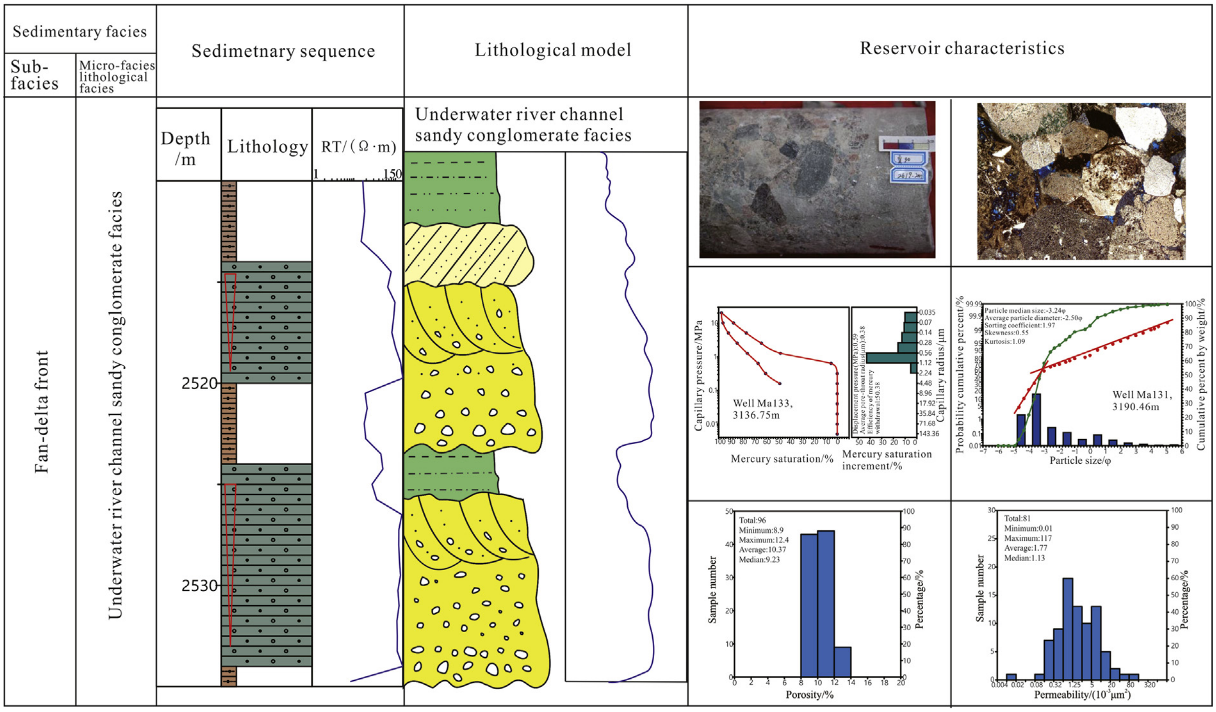

Fig. 7. Sedimentary characteristics of the underwater river course sandy conglomerate in the fan delta front.

sediments are mainly gray and gray to green conglomerate sandstone and sandstone. Compared to underwater main channel conglomerate microfacies, it has fewer conglomerate content, is mainly particle supported, and has relatively good roundness and poor sorting (sorting coefficient = 1.97). Large trough cross-bedding is developed locally in the middle sandy conglomerate layer with certain imbrication, and there is a small erosional surface that retains gravel and muddy gravel. The probability curve of the grain size shows a typical two-stage channel sediment style. The average particle size is −2.50φ, and median particle size is −3.24φ. Its resistivity curve is primarily a tooth- and bell-like shape with high

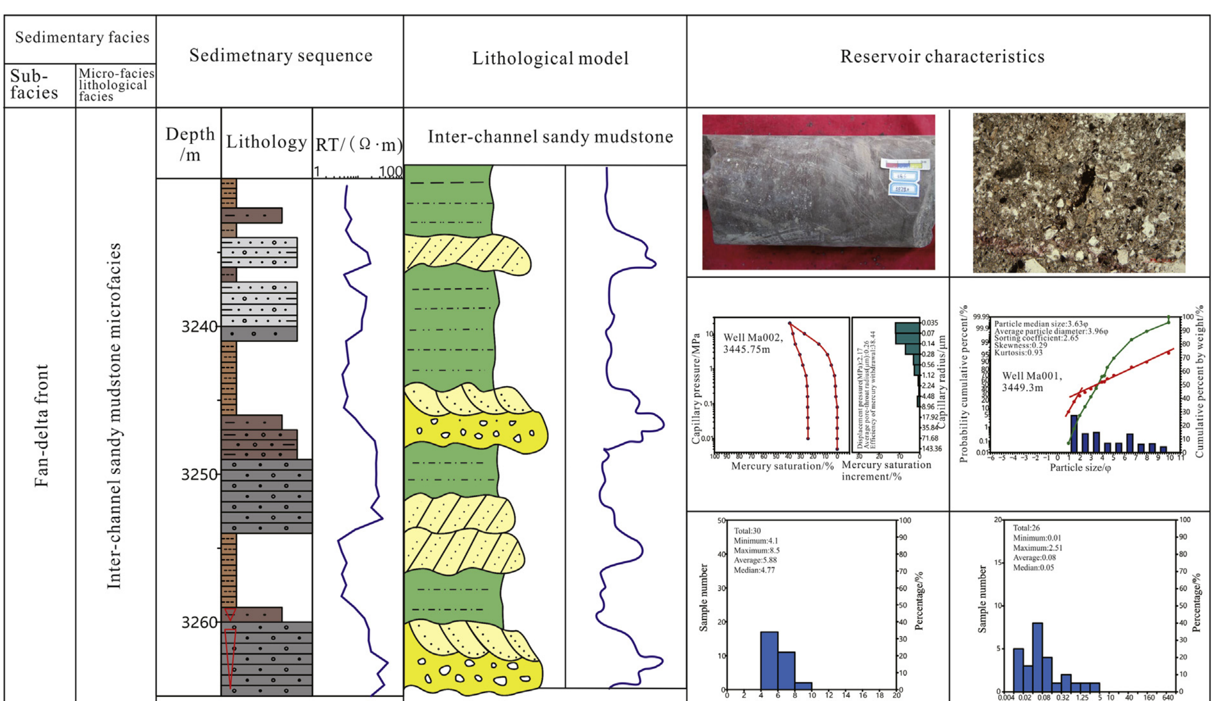

Fig. 8. Sedimentary characteristics of the underwater river inter-channel sandy mudstone microfacies in the fan delta front.

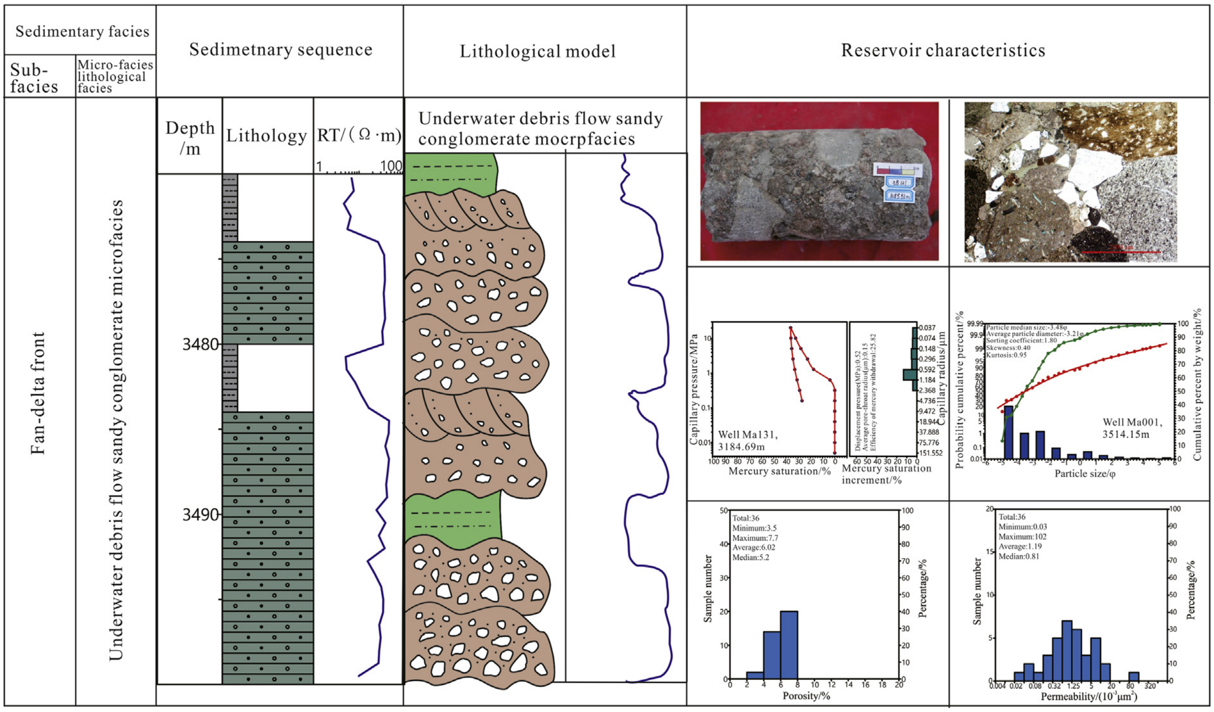

Fig. 9. Sedimentary characteristics of the underwater debris-flow sandy conglomerate microfacies in the fan delta front.

amplitude, and it can also form composite style with a bell-like shape on top of a box-like shape. The mercury intrusion curve shows that its displacement pressure is 0.59 MPa, the maximum connected pore-throat radius is 1.25 μm, averaging 0.38 μm, the medium pressure of saturation is 1.40 MPa, and the efficiency of mercury withdrawal is 50.38. The distribution of porosity for 96 core samples is relatively concentrated, ranging from 8.9% to 12.4%, and averaging 10.37%. The range of measured permeability for 81 samples is 0.01×10^{-3}-117×10^{-3} μm^2, with an average of 1.77×10^{-3} μm^2 (Fig. 7). Overall, the underwater channel sandy conglomerate facies in the fan delta front is a good

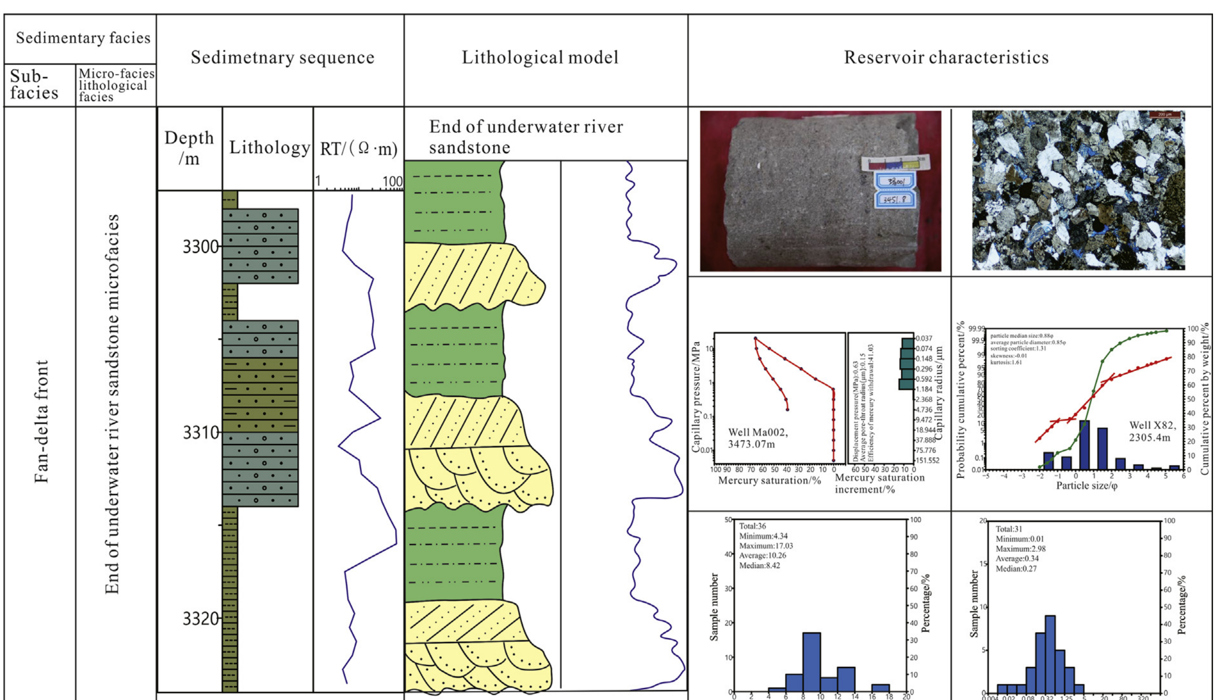

Fig. 10. Sedimentary characteristics of the end of the underwater channel in the fan delta front.

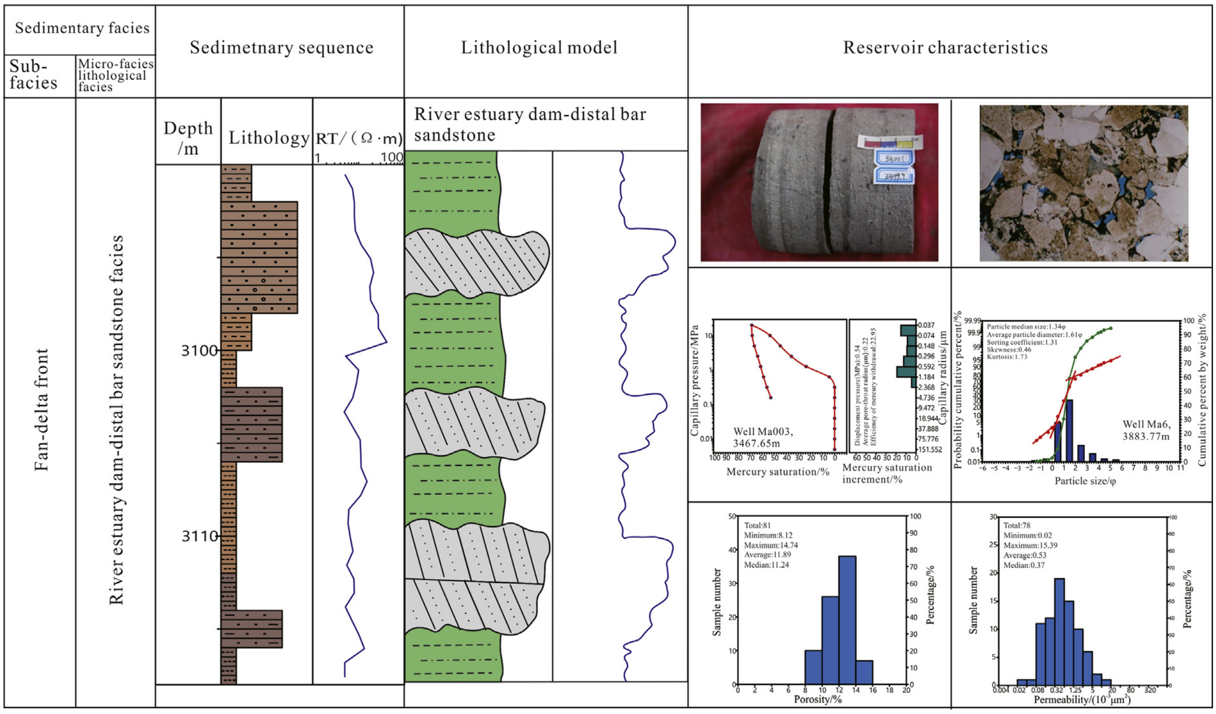

Fig. 11. Sedimentary characteristics of the river estuarial dam-distal bar sandstone microfacies in the fan delta front.

reservoir with a high efficiency of mercury withdrawal, relatively good porosity and high permeability.

4.6. Underwater river inter-channel sandy mudstone microfacies in the fan delta front

This microfacies develops between the underwater channels in the fan delta front. It is mainly gray green to gray, and has thin silty mudstone layers with horizontal sandy bedding or lenticular sandstone. Because of the strong erosion of underwater distributary channels and the frequent diversion, these sediments are generally thinned and washed away once the river is diverted. The probability curve of the grain size is a typical suspended one-stage style, and the medium grain size is 3.63 φ (average size = 3.96 φ) with relatively good sorting (the sorting coefficient = 2.65). The average porosity is 5.88%, and the average permeability is 0.08×10^{-3} μm^2. The displacement pressure is 2.17 MPa, and the efficiency of mercury withdrawal is 38.44. The resistivity curve is mostly tooth-shaped, finger-shaped, or tooth-finger-shaped (Fig. 8). Overall, this microfacies normally has poor quality reservoir rocks.

4.7. Underwater debris-flow sandy conglomerate microfacies in the fan delta front

The underwater debris-flow sandy conglomerate microfacies in the fan delta front is mainly a mixed deposition of gray and gray green conglomerate, sandy conglomerate, sandstone and mudstone. The sorting is relatively poor with high matrix content, and the roundness is moderate. The probability curve of the grain size is gentle with a small slope and concaved shape, which represents an overall jumping and slow transition of suspension without a significant turning point. All of the particles are in the suspension stage. The range of grain size is from −5φ to 5φ (the average size = −3.21φ; the median size = −3.48φ). The resistivity curve indicates a composite of a box-like shape and bell-like shape with moderate amplitude. The mercury intrusion curve shows that the average pore-throat radius is 0.15 μm, the displacement pressure is 0.52 MPa, and the efficiency of mercury withdrawal is 25.82. Overall, the underwater debris-flow sandy conglomerate microfacies has an averaged porosity of 6.02%, and the average permeability is 1.19×10^{-3} μm^2 (Fig. 9).

4.8. End of underwater river course sandstone microfacies in the fan delta front

The end of the underwater river course microfacies in the fan delta front is formed at the end of an underwater distributary channel in the fan delta front. It is mainly composed of well sorted, rounded gray moderate-coarse sandstone with conglomerates with low matrix content. Small trough-beddings and tabular beddings are common. The well logging curve is a bell- and finger-shape with moderate magnitude. The probability curve of the grain size is a jumping and suspension and transition style, which reflects the hydrodynamic characteristics of water flow energy decreasing when flowing into the lake basin during the normal water period. The mercury injection curve shows that the displacement pressure is 0.63 MPa, and the efficiency of mercury withdrawal is 41.03. The end of the underwater channel sandstone microfacies acts as good reservoir rocks, where the porosity and permeability conditions are relatively good with an average porosity of 10.26%, and an average permeability of 0.34×10^{-3} μm^2 (Fig. 10).

4.9. River estuary dam-distal bar sandstone microfacies in the fan delta front

The river estuary dam-distal bar sandstone microfacies in the fan delta front is an extension and product of the underwater distributary river towards the basin. It is composed of moderate-fine sandstone, siltstone or pebbly fine sandstone with cross-beddings and tabular beddings with low matrix content. Erosion surfaces are rare. They are made of fine to very fine, well sorted, well rounded sandstone and siltstone. The lithological and electrical properties exhibit anti-sequence deposition and the thick layer increases from downward to upward. The probability curve of the grain size is a typical three-stage style with a high slope. The sorting coefficient is 1.31, which indicates significant traction flow. The resistivity curve is tooth-funnel-shape with moderate amplitude. The mercury injection curve indicates that the discharge pressure is 0.54 MPa, and the average pore-throat radius is 0.22 μm. The efficiency of mercury withdrawal is 22.95. Overall, this microfacies has relatively high porosity and permeability, average is 11.89% and 0.53×10^{-3} μm^2 respectively (Fig. 11).

4.10. Silty sandstone microfacies in the pro-fan delta

Silty sandstone microfacies in pro-fan delta is located outside of the fan delta front (Fig. 12). It has the largest area and thickest deposition in the fan-delta system. The pro-fan

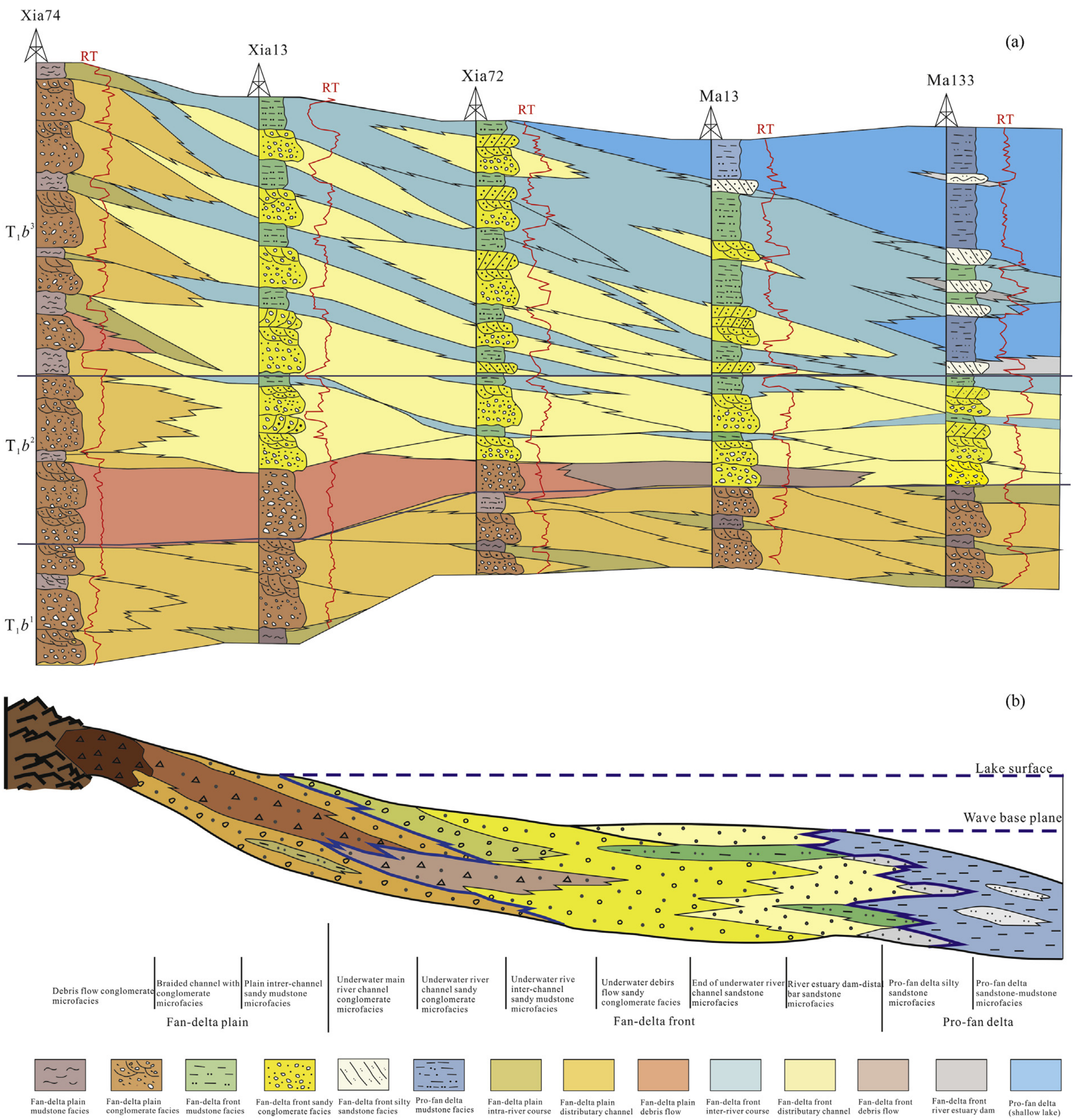

Fig. 12. Evolutionary characteristics (a) and sedimentary model (b) for the sedimentary facies of the northern Mahu Sag.

delta silty sandstone consists mostly of grey and gray-green siltstone and silty mudstone. The common sedimentary structures include ripple bedding and horizontal bedding. The roundness is well rounded to rounded; and sorting of siltstone is very good to good with a sorting coefficient of 1.21, which indicates sustained and stable hydrodynamic conditions. The probability curve of the grain size is a typical two-stage type, and its slope of the jumping component is relatively high. The resistivity curve is tooth- and finger-shaped with moderate magnitude. The mercury injection curve indicates that the average pore-throat radius is 0.31 μm, and the displacement pressure is relatively high at 1.15 MPa. The efficiency of mercury withdrawal is relatively poor (34.53). Overall, the porosity and permeability conditions are relatively poor with the average porosity at 5.52% and average permeability at 0.07×10^{-3} μm^2, indicating that this microfacies is not good reservoir of rocks (Fig. 13).

4.11. Fine sandstone-mudstone microfacies in the pro-fan delta

The pro-fan delta mudstone microfacies is located at the most frontward of the fan deltas. It is characterized by gray mudstone interbedded with thin argillaceous siltstone and fine sandstone (the average size = 3.95φ), with horizontal beddings. The sorting is good with high clay content. Its grain size probability curve is a two-stage type, which indicates that the hydrodynamic condition of the fan-delta front is relatively stable. It has a finger- or tooth-shape on the resistivity curve. Its mercury injection curve indicates that the displacement pressure of the front fan-delta mudstone facies is 6.75 MPa, and the average pore radius is close to 0 μm. It has no reservoir capacity; however, under certain conditions, it can be used as a good oil-generating rock layer or cap layer (Fig. 14).

5. Sedimentary facies model

Based on a detailed analysis of 11 sedimentary microfacies, we established a Triassic fan delta facies model in the Mahu Sag, northwestern margin of the Junggar Basin.

5.1. Facies characteristics and distribution

The sequence stratigraphy has significant control on the type, scale and continuity of sand bodies. Core observations and well-logging data provide good conditions for the study of strata and reservoirs. In general, when the same sedimentary facies is in different locations along the sequence cycles, the distribution patterns and physical properties of the sand bodies can be quite different [20,21]. In this paper, we selected a northeast-southwest cross-section from the piedmont to the center of the Mahu Sag to document sequence and facies characteristics within the Baikouquan Formation (Fig. 12). It covers the sub-facies of the fan-delta, including fan delta plain, fan delta front, pro-fan delta, and shore-shallow lacustrine sub-facies. Detailed sequence and facies in the Baikouquan Formation show that T_1b_1 mainly consists of fan-delta plain sub-facies. Overall, it shows normal grading with a fine-moderate conglomerate at the bottom and sandy conglomerate and conglomerate on the top. The T_1b_2 is the fan-delta front sub-facies that is developed in Well X13 and Well X72, and the fan-delta plain sub-facies in Well X74. The

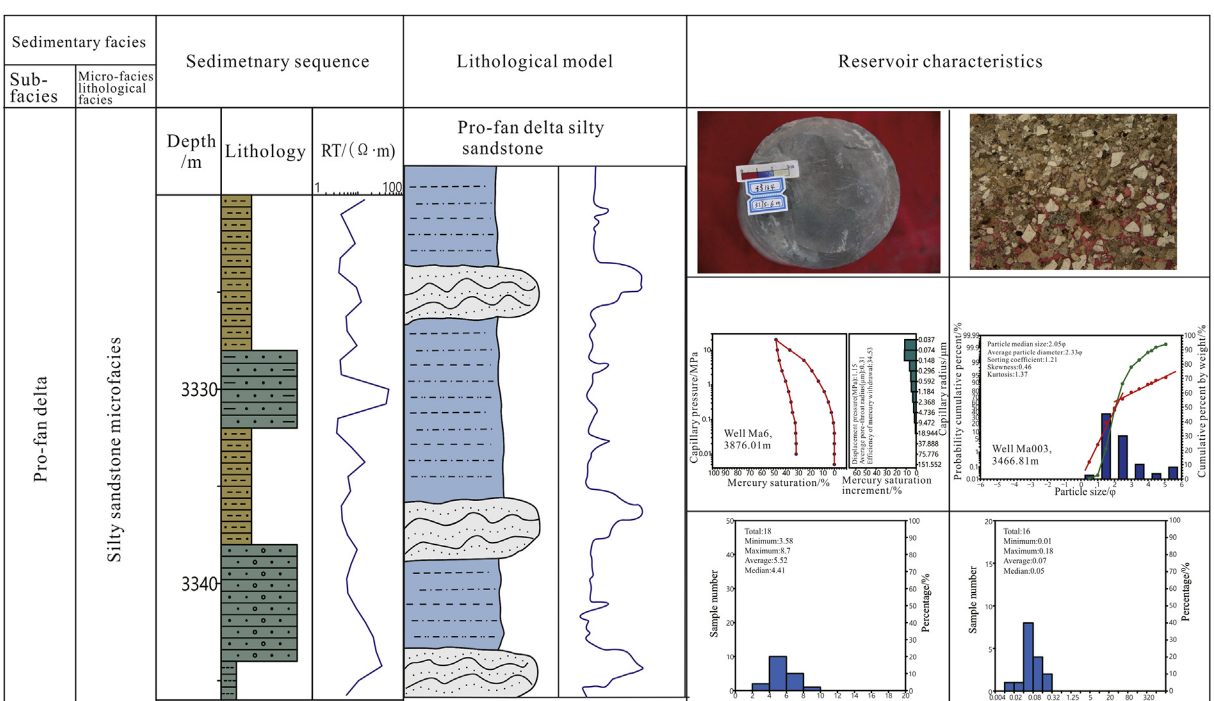

Fig. 13. Sedimentary characteristics of silty sandstone microfacies in the pro-fan delta.

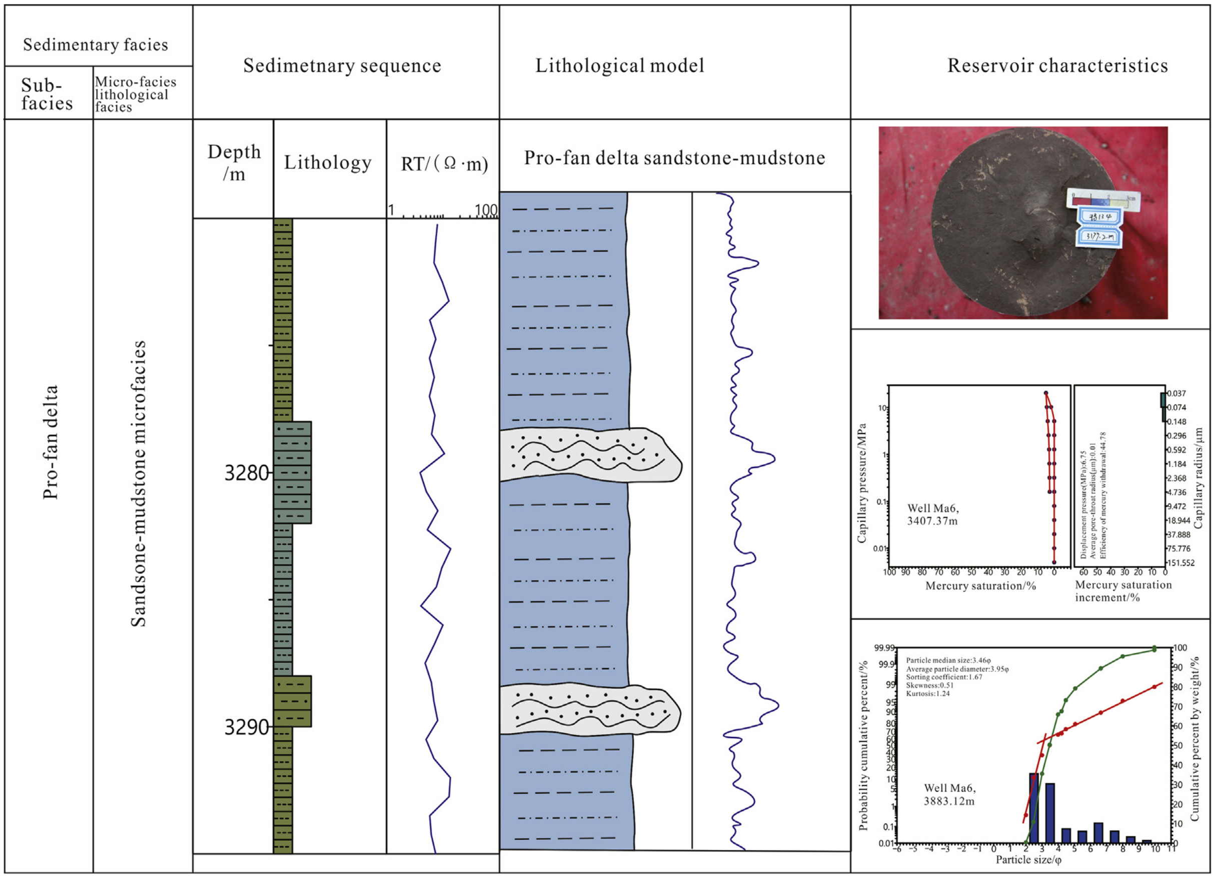

Fig. 14. Sedimentary characteristics of sandstone-mudstone microfacies in the pro-fan delta.

fan-delta front sub-facies consists of a lower fine conglomerate and sandy conglomerate with eroded contact and high-angle oblique bedding, a dark gray mudstone interlayer with horizontal bedding, and upper interbedded fine sandstone and silty sandstone with low-angle oblique bedding. In the T_1b_3, fan-delta front mudstone and silty sandstone facies develop in Well M13 and Well M133, fan-delta plain sub-facies develops in Well X74, and the fan-delta front develops in Well X13 and Well X72. The front fan-delta sub-facies is an interlayer of dark gray mudstone and silty sandstone with ripple bedding and horizontal bedding.

Detailed studies of facies of the Baikouquan Formation in single wells in the northern Mahu Sag suggest that the Triassic fan delta has retrogressive succession. From the source area to the basin center, it develops a sequential fan-delta plain, fan delta front, and pro-fan delta sub-facies. The cross section of wells show that the fan-delta plain sub-facies mainly develops in Wells X74, X13, X72, M13, and M133 during the first segment of the Baikouquan Formation, and the bottom of the second segment of the Baikouquan Formation in Wells X13 and X72 (Fig. 12a). In the complex microfacies of fan-delta plains, the gravity flow and braided distributary channel sand bodies are the two most important microfacies, forming the majority of sand bodies in the fan delta. The distributary river inter-channel sandy mudstone is the second important microfacies. At the bottom of the second segment of the Baikouquan Formation, the sandy conglomerate microfacies in fan delta plain formed by the sedimentary gravity flow are poorly sorted and characterized by a matrix-supported massive structure. The fan delta front sub-facies mainly develops in Wells X13 and X72 in the middle and upper part of the second segment, the third and second segment in Wells M13 and M133, and at the bottom of the third segment of the Baikouquan Formation. In the fan delta front sub-facies belt, the distributary river estuary dam-distal bar, distributary channel sandy conglomerate in the fan delta front, and underwater gravity flow deposits are important potential reservoirs. In the vertical direction, they normally form reverse grading with coarser sediment at the top.

5.2. Triassic sedimentary facies model in the northern Mahu Sag

The Triassic Baikouquan Formation of the Mahu Sag represents the fan delta of a lake transgressive retrogradational succession. Based on its lithology, sedimentary structure, cores, grain size, well-logging signatures, porosity and permeability data, we divided the fan delta into three sub-facies and 11 microfacies, and established a Triassic fan-delta depositional model of the Mahu Sag (Fig. 12b). This sedimentary model indicates the types of sedimentary systems that occur from the piedmont source to the lake center in the northern Mahu Sag along the northwestern margin of the Junggar Basin, and spatial distribution of sedimentary microfacies. Results can be potentially used to provide a theoretical basis for predictions of large-scale reservoirs.

6. Discussion

Based on core observations, sedimentary structure, thin section, particle size, signs of well-logging facies, porosity and permeability data, we defined 11 sedimentary microfacies for the fan delta in the research area and provided a detailed elaboration of their characteristics (Figs. 3−13). From the petrological characteristics and physical properties of these 11 sedimentary microfacies (Figs. 3−13), we can evaluate the differences of reservoir properties in different sedimentary microfacies of the Triassic Baikouquan Formation in the northern Mahu Sag; therefore, we can identify the microfacies distribution of favorable reservoirs. In addition, we compared the relationship between porosity and permeability for different sedimentary microfacies (Fig. 15).

To further reveal the distribution of sedimentary microfacies and their control of reservoirs, we plotted the sedimentary microfacies and reservoirs in the second segment of the Baikouquan Formation in the north slope of the Mahu Sag (Fig. 16). As shown in Fig. 15, the porosity of 11 microfacies from the fan-delta facies in northern Mahu Sag is mainly concentrated at 4%−14%, and the permeability is mainly at 0.1×10^{-3}−100×10^{-3} μm^2. In addition, there is a positive correlation between porosity and permeability, which indicates the reservoir space is mainly made of original intergranular pores, and diagenesis has a strong relationship with the reservoir's physical property [22−24]. Additionally, the cross plot of porosity and permeability has a relative concentration, which reveals that sedimentary microfacies may show a stronger impact on the reservoir property than diagenesis [25]. According to Fig. 16, the fan-delta plain sub-facies of the second segment of the Baikouquan Formation is mainly distributed in the area of X25-X10-X15-M5. The physical properties of the braided channel microfacies with sandy conglomerate in the fan-delta plain sub-facies are relatively good. The average porosity is 10.78%, and the average permeability is 14.07×10^{-3} μm^2. This could be due to a relatively shallow burial at approximately 2000 m and relatively weak compaction [26]. The preservation of primary pores is relatively complete; therefore, the porosity and permeability are relatively good. Although this microfacies has relatively good physical properties and is near the margin of the lake and piedmont, there is no indication of hydrocarbon in the braided channel sandy conglomerate microfacies for the perspective of exploration. One of the possible reasons is that the structural location in the upper nappe structure [3,19] is not favorable for the migration and accumulation of hydrocarbon. As a result, they are not favorable zones for reservoir microfacies although they have relatively good physical properties.

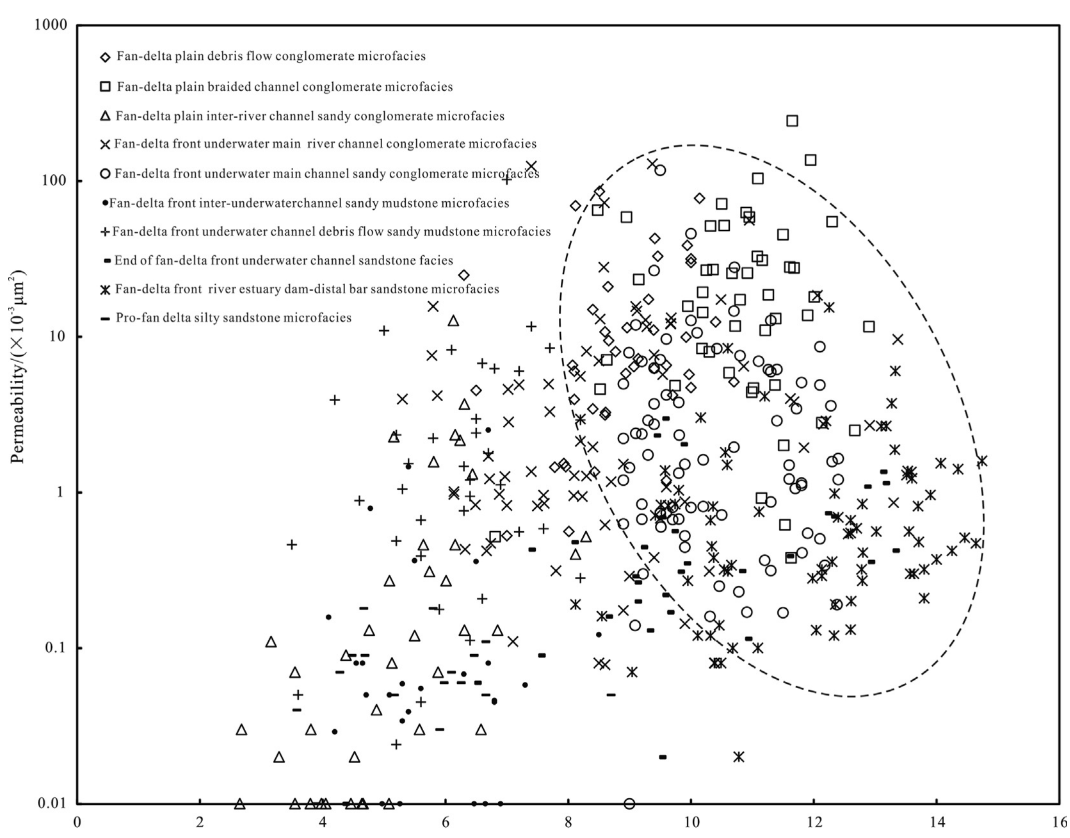

Fig. 15. Permeability Correlation diagram between porosity and permeability from various sedimentary microfacies.

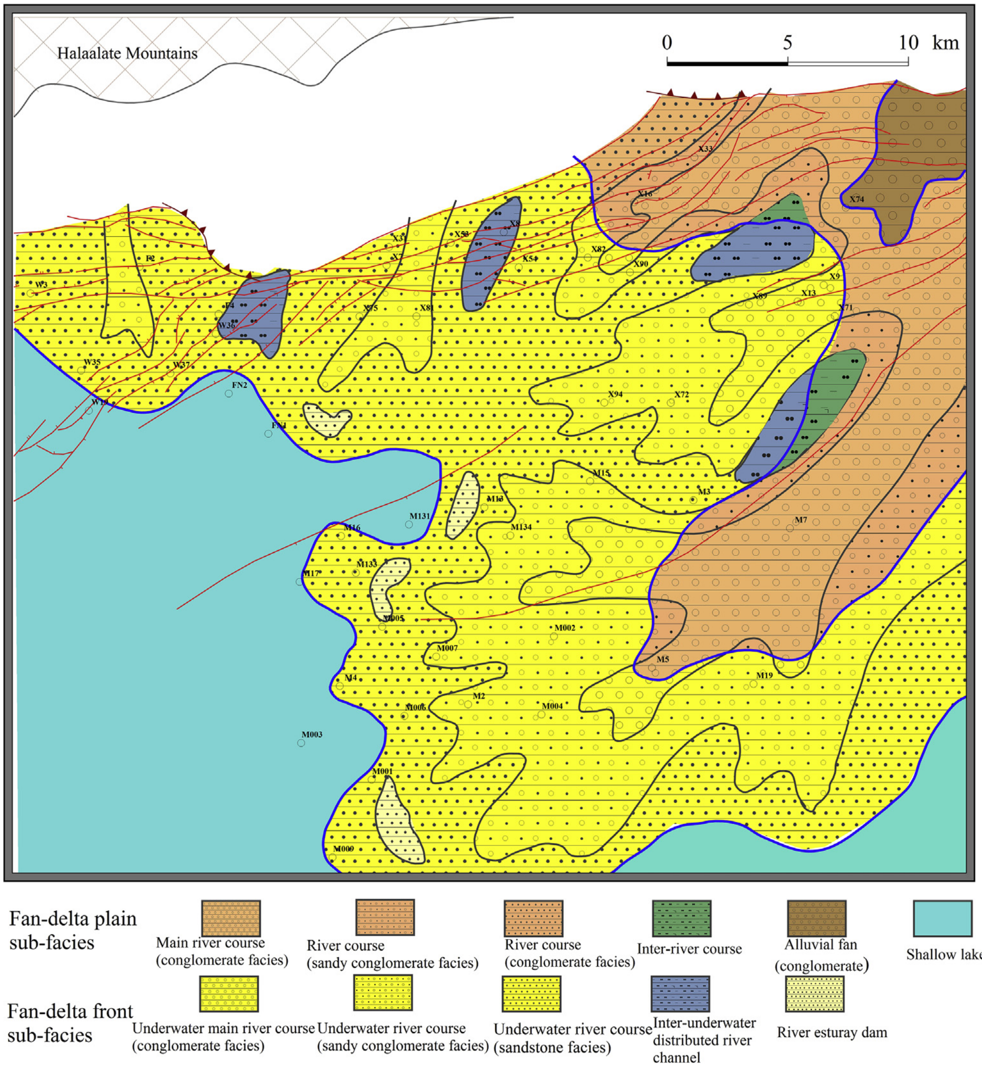

Fig. 16. Planar distribution of the sedimentary microfacies and reservoirs in the second segment of the Baikouquan Formation in the northern Mahu Sag.

The sub-facies of the fan delta front in the second segment of the Baikouquan Formation is mainly distributed in the area of W35-FN4-M2-M4. The average porosity of the underwater river course microfacies with sandy conglomerate in the fan delta front is 10.37%, and the average porosity of the river estuary dam-distal bar sandstone is 11.89%. The porosity is relatively high, and its river course has relatively good physical properties that are mostly favorable for reservoir rocks in the fan-delta facies. For this sedimentary microfacies, under relatively stable hydrodynamic conditions, the conglomerate has been washed and shows a relatively high compositional maturity with little muddy matrix content; thus, it has the highest quality of reservoirs.

The average porosity is 9.06% in the main river course microfacies with sandy conglomerate rock of the fan-delta plain, debris-flow microfacies with sandy conglomerate, and the underwater main river course conglomerate microfacies in the fan delta front sub-facies; the average porosity of the sandstone at the end of the underwater river course is 10.26%. These microfacies show a relatively weak washing effect, and the compositional maturity is relatively low with stronger compaction than fan delta plain sub-facies. In addition, the dissolution is not sufficiently developed or seldom happens. Therefore, this microfacies is a low quality reservoir in comparison with those conglomerate reservoirs within the fan delta front microfacies. Similarly, the physical properties of alluvial fans, inter-channel in the fan-delta plain, inter-channel in the fan delta front and the silty sandstone microfacies in the front fan delta are relatively poor, and they are not effective reservoirs.

In summary, the hydrocarbon exploration focus should be placed in the area of the fan delta front. In addition, attention should be paid to the braided distributary channel sand body in the fan-delta plain. The amount of development is relatively small, but the size of a single body is relatively large, and its physical properties are relatively good. Triassic fan-delta sedimentary microfacies in the Mahu Sag show important implications for exploration in the Xinjiang Oilfield. This model can help explore the "fan-controlled" hydrocarbon reservoirs in the northwestern margin of the Junggar Basin and similar settings in other basins.

7. Conclusions

The main conclusions from this study include:

(1) The Triassic Baikouquan Formation of the Mahu Sag represents the fan delta of a lake transgressive retrogradational succession. Based on its lithology, sedimentary structure, cores, grain size, well-logging signatures, porosity and permeability data, we divided the fan delta into three sub-facies and 11 microfacies (lithofacies), and established a Triassic fan-delta depositional model of the Mahu Sag.
(2) The underwater river course microfacies in the fan delta front with conglomerate, estuary dam and distal bar sandstone microfacies are the mostly favorable reservoir facies belts; the fan-delta plain braided channel microfacies in the fan delta plain with conglomerate, debris-flow microfacies with conglomerate, underwater main channel microfacies with conglomerate in the fan delta front and the end of underwater river course microfacies with sandstone are relatively favorable reservoir facies belts.
(3) The underwater debris-flow conglomerate microfacies and front fan-delta silty sandstone microfacies are reservoir facies belts as additional reserves; the underwater river interchannel microfacies with sandstone, mudstone, sand-shale facies between fan-delta plain river interchannel microfacies with sandstone-mudstone, and front fan-delta mudstone microfacies have limited reservoir properties.

Funding

Supported by China National Science & Technology Major Project (2011ZX05000-01-06); National Basic Research Program of China (973 Program) (2011CB201104); 2012 Western Doctor Foundation of the Chinese Academy of Sciences; Special Funding for Key Laboratories of Gansu Province (1309RTSA041); Foundation of Key Laboratory of Mineral Resources in Western China (Gansu Province); Lanzhou University and Science and Technologic Plan for Jiayuguan City.

Conflict of interest

The authors declare no conflict of interest.

Acknowledgements

We acknowledge the Xinjiang Oilfield Company of the China National Petroleum Co. Ltd. for providing cores, logging data, and analyses of the physical properties, and we also acknowledge Zhongke Lianheng Inc. for providing the software Geores, which was used to process the data for the granularity, mercury injections, and physical properties and plot graphics.

References

[1] X. Lu, X. Xie, S. Zhang, A.B. Busbey, S. Zhang, S. Du, G. Sun, J. Shi, U-Pb detrital zircon geochronology of Late Triassic to Early Jurassic sandstones in the northwestern Junggar Basin and its implications, J. Geol. Geophys. 7 (1) (2017) 1000320.
[2] Z. Cai, F. Chen, Z. Jian, Types and tectonic evolution of Junggar Basin, Earth Sci. Front. 7 (2000) 431–440.
[3] D. He, C. Yin, S. Du, X. Shi, H. Ma, Characteristics of structural segmentation of foreland thrust belts—a case study of the fault belts in the northwestern margin of Junggar Basin, Earth Sci. Front. 11 (2004) 91–101.
[4] B. Ren, J. Qu, W. Zesheng, H. Qian, Y. Tang, Hierarchical control function of the paleogeomorphology in triassic Period to sedimentary in Mahu sag, J. Southwest Pet. Univ. (Sci. Technol. Ed.) 38 (2016) 81–89.
[5] D. Lei, J. Qu, Z. An, X. You, T. Wu, Hydrocarbon accumulation conditions and enrichment regularity of low-permeability glutenite reservoirs of Baikouquan Formation in Mahu Sag, Junggar Basin, Xinjing Pet. Geol. 36 (2015) 642–647.
[6] Y. Yu, D. Li, S. Hu, Z. Lei, D. He, Fan sedimentation and exploration direction of fan hydrocarbon reservois in forland thrust belt of the northwestern Junggar Basin, Acta Geosci. Sin. 28 (2007) 62–71.
[7] Z. Lei, D. Bian, S. Du, Y. Yu, H. Ma, Characteristics of fan forming and oil gas distribution in west north margin of Junggar Basin, Acta Pet. Sin. 26 (2005) 8–12.
[8] C. Zou, L. Hou, L. Kuang, J. Kuang, Genetic mechanism of diagenesis-reservoir facies of the fan-controlled Permo-Triassic in the western margin area, Junggar Basin, Chin. J. Geol. 42 (2007) 587–601.
[9] X. Lu, Y. Kong, J. Chang, J.A. Shi, S. Zhang, Characteristics and main controlling factors of sand gravel stone reservoir of permian fencheng formation in Kebai area, northwest Junggar Basin, Nat. Gas Geosci. 23 (2012) 474–481.
[10] X. Lu, J. Shi, S. Zhang, The characteristic of sand-gravel stone reservoir and the analysis of prime controlling factors in Permian Fengcheng Formation at Kebai area, Junggar Basin, Int. J. Adv. Inf. Sci. Serv. Sci. 4 (2012) 611–619.
[11] D. Li, D. He, Y. Lian, Y. Lu, Z. Yi, Structural evolution and late carboniferous magmatism of the Zhongguai arc in the western Junggar Basin, northwest China: implications for tectonic evolution of the Junggar ocean, Int. Geol. Rev. 59 (2016) 1234–1255.
[12] J. Kuang, X. Qi, The structural characteristics and oil-gas explorative direction in Junggar foreland basin, Xinjing Pet. Geol. 27 (2006) 5–9.
[13] T. Wu, Genetic Mechanism Study of Favorable Reservoir in Baikouquan Formation of Triassic in the Slope Area of Mahu Depression, Junggar Basin, Lanzhou Center for Oil and Gas Resources, Insititute of Geology and Geophysics, CAS, Chinese Academy of Scienses, Lanzhou, 2014, p. 99.
[14] X. Chen, L. Nie, W. Ding, X. Wang, Z. Wang, B. Ye, The relationship between strike-slip tectonic system and geochemical anomalies in the west Junggar, northwestern China and its implication for mineral exploration, Acta Petrol. Sin. 31 (2015) 371–387.
[15] F. Chen, X. Wang, X. Wang, Prototype and tectonic evolution of Junggar Basin, northwestern China, Earth Sci. Front. 12 (2005) 77–89.
[16] B. Chen, B.M. Jahn, Genesis of post-collisional granitoids and basement nature of the Junggar Terrane, NW China: Nd-Sr isotope and trace element evidence, J. Asian Earth Sci. 23 (2004) 691–703.
[17] W. Yao, B. Li, S. Zhang, J. Shi, Characteristics of Permian-Carboniferous volcanic reservoir in Zhongguai-Wuba area in northwestern margin of Junggar Basin, Lithol. Reservoirs 23 (2011) 46–52.
[18] G. Chen, Ablimit, L. Bai, J. Zhang, B. Bian, Petroleum accumulation field in deep strata of the eastern slope area of the Mahu Sag, Junggar Basin, J. Southwest Petrol. Univ. (Sci. Technol. Ed.) 35 (2013) 31–38.
[19] G. Zhang, W. Yang, Tectonic characteristics of overthrust fault belt and looking for oil zone in Karamay, Xinjiang Geol. 4 (1983) 1–5.
[20] M.A. Zahid, C. Dong, C. Lin, J. Gluyas, S. Jones, X. Zhang, M.J. Munawar, C. Ma, Sequence stratigraphy, sedimentary facies and reservoir quality of Es_4s, southern slope of Dongying Depression, Bohai Bay Basin, East China, Mar. Petrol. Geol. 77 (2016) 448–470.

[21] F. Lu, X. Tan, T. Ma, L. Li, A. Zhao, C. Su, J. Wu, H. Hong, The sedimentary facies characteristics and lithofacies palaeogeography during Middle-Late Cambrian, Sichuan Basin and adjacent area, Petroleum 3 (2017) 212−231.

[22] G. Xu, P. Zhang, F. Xu, X. Wang, C. Yang, Diagenesis and pore evolution of cretaceous tugulu group reservoir in chepaizi, Junggar Basin, China, J. Chengdu Univ. Technol. (Sci. Technol. Ed.) (2015) 513−520.

[23] S. Dong, M. Shalaby, M. Islam, Integrated reservoir characterization study of the McKee Formation, Onshore Taranaki Basin N. Z. Geosci. 8 (2018), https://doi.org/10.3390/geosciences8040105.

[24] P.H. Nelson, J.E. Kibler, Permeability-porosity relationships in sedimentary rocks, Log. Anal. 35 (1994) 38−62.

[25] K.W.O.B. Knox, W.G. Burgess, K.S. Wilson, A.H. Bath, Diagenetic influences on reservoir properties of the sherwood sandstone (Trisaaic) in the marchwood geothermal borehole southampton, UK, Clay Minierals 10 (1984) 441−456.

[26] X. Lu, Y. An, W. Xia, Z. Hu, S. Zhang, J. Shi, The characteristics and reservoir-controlling of sedimentary facies of Jurassic Sangonghe formation at east Fukang slope, Junggar Basin, Nat. Gas Geosci. 28 (2017) 1810−1820.